© 1999 Oxford University Press
Nucleic Acids Research, 1999, Vol. 27, No. 17 **3583–3588**

Magnesium-dependent alternative foldings of active and inactive *Escherichia coli* tRNA^{Glu} revealed by chemical probing

Eric Madore, Catherine Florentz[1], Richard Giegé[1] and Jacques Lapointe*

Département de Biochimie, Faculté des Sciences et de Génie, Université Laval, Québec G1K 7P4, Canada and [1]Laboratoire de Biochimie, Institut de Biologie Moléculaire et Cellulaire du CNRS, 15 rue René Descartes, F-67084 Strasbourg Cedex, France

Received April 2, 1999; Revised and Accepted July 8, 1999

ABSTRACT

A stable conformer of *Escherichia coli* tRNA^{Glu}, obtained in the absence of Mg^{2+}, is inactive in the aminoacylation reaction. Probing it with diethylpyrocarbonate, dimethyl sulfate and ribonuclease V1 revealed that it has a hairpin structure with two internal loops; the helical segments at both extremities have the same structure as the acceptor stem and the anticodon arm of the native conformer of tRNA^{Glu} and the middle helix is formed of nucleotides from the D-loop (G15–C20:2) and parts of the T-loop and stem (G51–C56), with G19 bulging out. This model is consistent with other known properties of this inactive conformer, including its capacity to dimerize. Therefore, this tRNA requires magnesium to acquire a conformation that can be aminoacylated, as others require a post-transcriptional modification to reach this active conformation.

INTRODUCTION

There is increasing information showing that the architectural characters of a macromolecule are not entirely imprinted in their genome sequences. Prions and chaperone-directed folding are typical examples in the protein field (1). Alternative conformations have been described in the RNA world and recently the importance of modified nucleotides for proper folding has been highlighted (2). Several pieces of evidence in older literature argue in favor of the existence of magnesium-dependent alternative conformations for tRNAs. Here we investigate this possibility by chemical structure probing of active versus inactive tRNA^{Glu} from *Escherichia coli*.

The acceptor activity of several tRNAs for their cognate amino acid is unexpectedly low following their purification, but is markedly increased after preincubation in the presence of magnesium ions (3). Their inactivity in the aminoacylation reaction was attributed to the denatured conformation of these tRNAs, including tRNA^{Trp}, tRNA^{His} and tRNA^{Glu} from *E.coli* and tRNA^{Ser}, tRNA^{Phe}, tRNA^{Met}, tRNA^{Arg}, tRNA^{Glu}, tRNA^{Ala} and tRNA^{Lys} from *Saccharomyces cerevisiae* (4–8). The so-called 'denatured conformer' of *E.coli* tRNA^{Glu} is the most extensively studied of these inactive tRNAs. As it is separated from the native form during chromatography on DEAE–Sephadex, it was initially believed that two tRNA^{Glu} isoacceptors were present in *E.coli* (9), but it was shown later that the so-called tRNA$_1^{Glu}$ is the 'denatured' conformer of the so-called tRNA$_2^{Glu}$ (10). This conclusion was strengthened by the fact that the *E.coli* genome contains four genes for tRNA^{Glu} and that their structural parts are identical (11). This 'denatured' conformer can regain its acceptor activity for glutamate by incubation with magnesium. Reciprocally, removing magnesium from the active tRNA leads to formation of the 'denatured' conformer (10,12).

Information on the structure of this denatured conformer has been obtained by various techniques (12): its mobility is greater than that of the native conformer during electrophoresis on polyacrylamide gels, its UV absorbency indicates that it contains only slightly fewer stacked bases than does the native one, it forms a dimer with tRNA^{Phe} as efficiently as does native tRNA^{Glu}, which indicates that it contains the anticodon loop with the anticodon bases stacked as in the native conformer, and at low temperature the 'denatured' conformer dimerizes when magnesium is added. Finally, relaxation kinetics experiments (13) suggested that the denatured conformer possesses only three helices and that these are the acceptor, the anticodon and possibly the T-stem.

We report here the characterization of this inactive conformer of *E.coli* tRNA^{Glu}. Probing it with dimethyl sulfate (DMS), diethylpyrocarbonate (DEPC) and RNase V1 revealed that its structure is the same as that of the native conformer for the acceptor stem and the anticodon stem and loop, but is totally different for the central region. As it possesses a defined structure, we will refer to it as an inactive instead of a denatured conformer.

MATERIALS AND METHODS

DMS was purchased from ACP Chemical Inc. DEPC, hydrazine and aniline were from Sigma. T4 polynucleotide kinase was from Pharmacia. Purification of the fully modified form of *E.coli* tRNA^{Glu} from an overproducing strain containing the pKR15 plasmid (kindly provided by Dr Kelley Rogers and Dr Dieter Söll) was performed as described by Madore *et al.* (manuscript in preparation) on a trioctylammonium-coated C_{18}

*To whom correspondence should be addressed. Tel: +1 418 656 2131; Fax: +1 418 656 3664; Email: jacques.lapointe@bcm.ulaval.ca

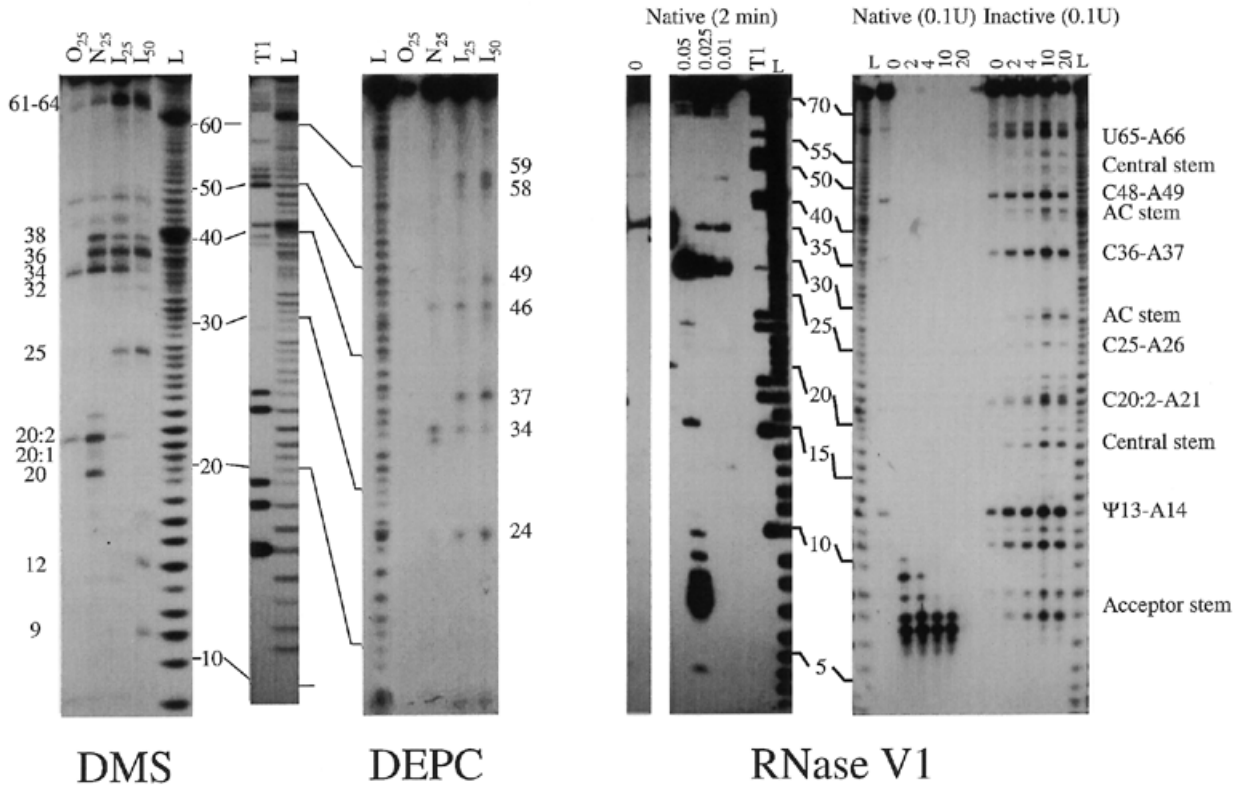

Figure 1. DMS, DEPC and RNase V1 probing of the native and inactive forms of *E.coli* $tRNA^{Glu}$. Digestions with DMS and DEPC were performed at pH 7.2 for 10 min. Digestion with RNase V1 was performed with 0.1 U of enzyme at pH 7.5 for periods of 0, 2, 4, 10 and 20 min and for the native form digestion was also performed with 0.01, 0.025 and 0.05 U of enzyme for 2 min. Fragments were separated by electrophoresis in a 12% polyacrylamide gel and visualized by autoradiography. L, alkaline ladder; T1, G ladder obtained from RNase T1 digestion; O, no DMS nor DEPC; N_{25}, active tRNA tested under native conditions at 25°C; I_{25}, inactive tRNA tested at 25°C; I_{50}, inactive tRNA tested at 50°C. Small differences between the ladder and the size of the fragments come from mobility changes due to the DMS and DEPC treatments. For the RNase V1 panel, fragile pyrimidine–A bonds and major cleavage sites are indicated.

ODS-Hypersyl column (14). Modified nucleotide content was verified by 2-dimensional thin layer chromatography (15,16). Pure $tRNA^{Glu}$ was 5'-^{32}P-end-labeled by T4 polynucleotide kinase and repurified by electrophoresis on a 15% polyacrylamide gel in the presence of 8 M urea.

Inactive (I) and native (N) forms of $tRNA^{Glu}$ were obtained by heating for 2 min at 60°C in 50 mM sodium cacodylate, pH 7.2, with, respectively, 1 mM EDTA and 10 mM $MgCl_2$ and letting the solution cool down for 20 min at room temperature (12). The $tRNA^{Glu}$ dimer was obtained by adding 1 mM $MgCl_2$ to the inactive tRNA at 0°C (12). Reactions with DMS and DEPC were performed as described by Romby *et al.* (17) at 25°C (10 min) for the native conformer, at 25 and 50°C (10 min) for the inactive one and at 4°C (20 min) for the dimer. RNase V1 assay (18) was performed using [^{32}P]$tRNA^{Glu}$ (100 000 c.p.m.), 40 mM Tris–HCl pH 7.5, 40 mM NaCl, 0.3 mM $MgCl_2$ and 0.1 U of RNase (or 10 mM $MgCl_2$ and 0.01, 0.025 and 0.05 U for the native form) in 20 µl. The reaction was stopped by the addition of 20 µl of a solution containing 0.6 M Na acetate, 4 mM EDTA and 0.1 µg/µl of total tRNA. tRNA samples were extracted with phenol and precipitated with ethanol. In all cases, fragments were separated by electrophoresis in a 12% polyacrylamide gel in the presence of 8 M urea and visualized by autoradiography.

Prediction of secondary structures was made using the Web version of the *mfold* software v.3.0 by Michael Zuker (Washington University School of Medicine) (19) (http://www.ibc.wustl.edu/~zuker/rna/form1.cgi).

RESULTS AND DISCUSSION

Chemical probing of the accessible cytosines and adenosines of $tRNA^{Glu}$

Cytosines that are not involved in Watson–Crick base pairs in *E.coli* $tRNA^{Glu}$ were identified by reaction with DMS, which attacks the accessible N^3 atoms of these nucleotides (20). In the native conformer of this fully modified $tRNA^{Glu}$ (see Materials and Methods), C20, C20:1, C20:2, mnm^5s^2U34, C36 and C38 are susceptible to DMS attack (Fig. 1, DMS lane N_{25}), which is consistent with its theoretical tertiary structure where all these nucleotides are in loops (Fig. 3A). Position 34 susceptibility is caused by hydrazinolysis, which can occur on modified nucleotides (20). In the inactive conformer, C36 and C38 are reactive but residues 20, 20:1 and 20:2 are not (Fig. 1, DMS

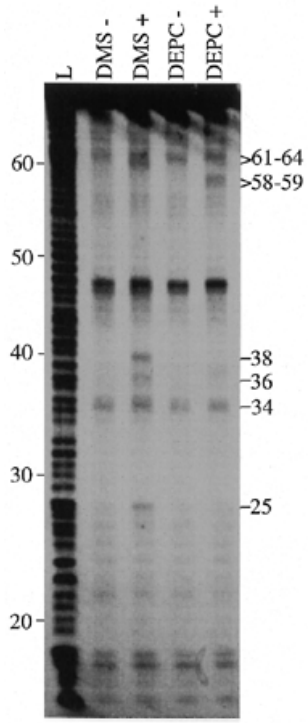

Figure 2. DMS and DEPC probing of the dimeric form of *E.coli* $tRNA^{Glu}$. Probing was performed at pH 7.2 for 20 min at 4°C. L, alkaline ladder. DMS– and DEPC– are negative controls.

lane I_{25}) and two bands corresponding to C25 and residues near position 62 are present; the latter is broad and may include cytosines from positions 61 to 64. At 50°C under denaturing conditions, two new bands appear at positions 9 and 12 (Fig. 1, DMS lane I_{50}) and may be attributed to tertiary structure melting. In the dimer (Fig. 2), C25, C36, C38 and C61–C64 are cleaved.

Adenines that are not stacked nor involved in the tertiary structure of $tRNA^{Glu}$ were identified using DEPC, which attacks their accessible N^7 atoms (20). In the native conformer, A46 and mnm^5s^2U34 were cleaved (Fig. 1, DEPC lane N_{25}). Position 34 was cleaved for the same reason as for its cleavage with DMS. From the tertiary structure model of $tRNA^{Glu}$ (Fig. 3A), drawn by analogy with the yeast $tRNA^{Phe}$ structure, we expected to see cleavage at A16 because it is not stacked and not likely to be involved in a tertiary interaction. The fact that this nucleotide is protected indicates novel features. For the inactive molecules, at 25 and at 50°C, new bands appear at positions 24, 37, 49, 58 and 59 (Fig. 1, DEPC lanes I_{25} and I_{50}), indicating that these nucleotides are no longer stacked (thus not in a stem) nor involved in the tertiary structure. In the dimer (Fig. 2), only A37 (slightly), A58 and A59 are reactive. The strong band observed around position 46 in the dimer, which also appears in the control experiments as well as in those performed in the presence of the probes, should be noted. These bands thus correspond to strong degradation of the tRNA. Such degradation, likely initiated at the level of the more sensitive pyrimidine–A linkages (21) at nucleotides U44–A46 and C48–A49, is not observed in the monomeric form of the tRNA and thus may reflect a local conformational change induced by dimer formation enhancing the exposure of domain 44–49 to the solvent.

Enzymatic probing with RNase V1

RNase V1 preferentially cleaves double-stranded RNA (18). The native and inactive forms of *E.coli* $tRNA^{Glu}$ differ markedly in their susceptibility to this nuclease (Fig. 1, RNase V1); after 2 min incubation with 0.1 U of RNase V1, native $tRNA^{Glu}$ is extensively digested, whereas the inactive form is much less cleaved. Strikingly, under such conditions all molecules of native $tRNA^{Glu}$ are digested while a significant amount of inactive $tRNA^{Glu}$ remains intact. With 10 times less enzymatic probe (0.01 U of RNase V1) we observed that the native form is predominantly cleaved at nucleotide 29 in the anticodon stem and around nucleotide 67 in the acceptor stem. For the inactive form, most of the signals come from fragile pyrimidine–A bonds and are also present at time 0, but some RNase V1-specific signals are observed at positions 7, 8, 18, 19, 21, 22, 27, 28, 29, 42, 43, 44, 53, 54 and 56 (the underlined positions correspond to stronger cleavage).

Structure of the inactive conformer of $tRNA^{Glu}$

Taking into account the fact that C25, C36, C38, C61, C62, C63 and C64 and A24, A37, A46, A49, A58 and A59 are accessible in the inactive conformer of $tRNA^{Glu}$ and that C20, C20:1 and C20:2 are not, we used the *mfold* software (19) to identify the most stable secondary structure that can satisfy these constraints. We obtained a hairpin-like structure with an estimated ΔG of –27.4 kcal/mol (which is close to the –28.7 kcal/mol calculated for native $tRNA^{Glu}$ at 37°C). The free energy difference between the most stable structure (our model) and the next best and significantly different one is ~10 kcal/mol. Therefore, using the constraints obtained by chemical probing, an essentially unique folding is obtained for inactive *E.coli* $tRNA^{Glu}$. Those ΔG values do not account for tertiary interactions nor for the presence of Mg^{2+}. This hairpin with two internal loops (Fig. 3B) can account for all the cleavages obtained with DMS and DEPC. The model is consistent with the digestion pattern observed with RNase V1: positions 18, 19, 53, 54 and 56 are in the central stem and 27, 28, 29, 42, 43 and 44 are in the anticodon loop. The marked difference in susceptibility to RNase V1 between the active and inactive forms of $tRNA^{Glu}$ may come from the length of the helices. The helices in the native form have 10 and 12 bp and are longer than those in our model for the inactive form (only 6 and 7 bp). Knowing that the minimal substrate length for RNase V1 is 4–6 bp (18), the latter is just on the limit and may not be as good a substrate as a 10 bp helix.

The presence of three helices agrees with the relaxation kinetics results of Bina-Stein *et al*. (13). This model also accounts for the RNase T1 results obtained by Wrede *et al*. (22). They observed that G22 and G23 were more sensitive in the inactive form than in the active one and that G18 and G19 were less reactive in the inactive $tRNA^{Glu}$. As RNase T1 preferentially cleaves G in single-stranded RNA, this result suggests that in the inactive form G22 and G23 are in a single-stranded region and G18 and G19 are in a stem, as in our model (Fig. 3B). The fact that DMS-induced cleavages at C20, C20:1 and C20:2 totally disappear in the absence of magnesium

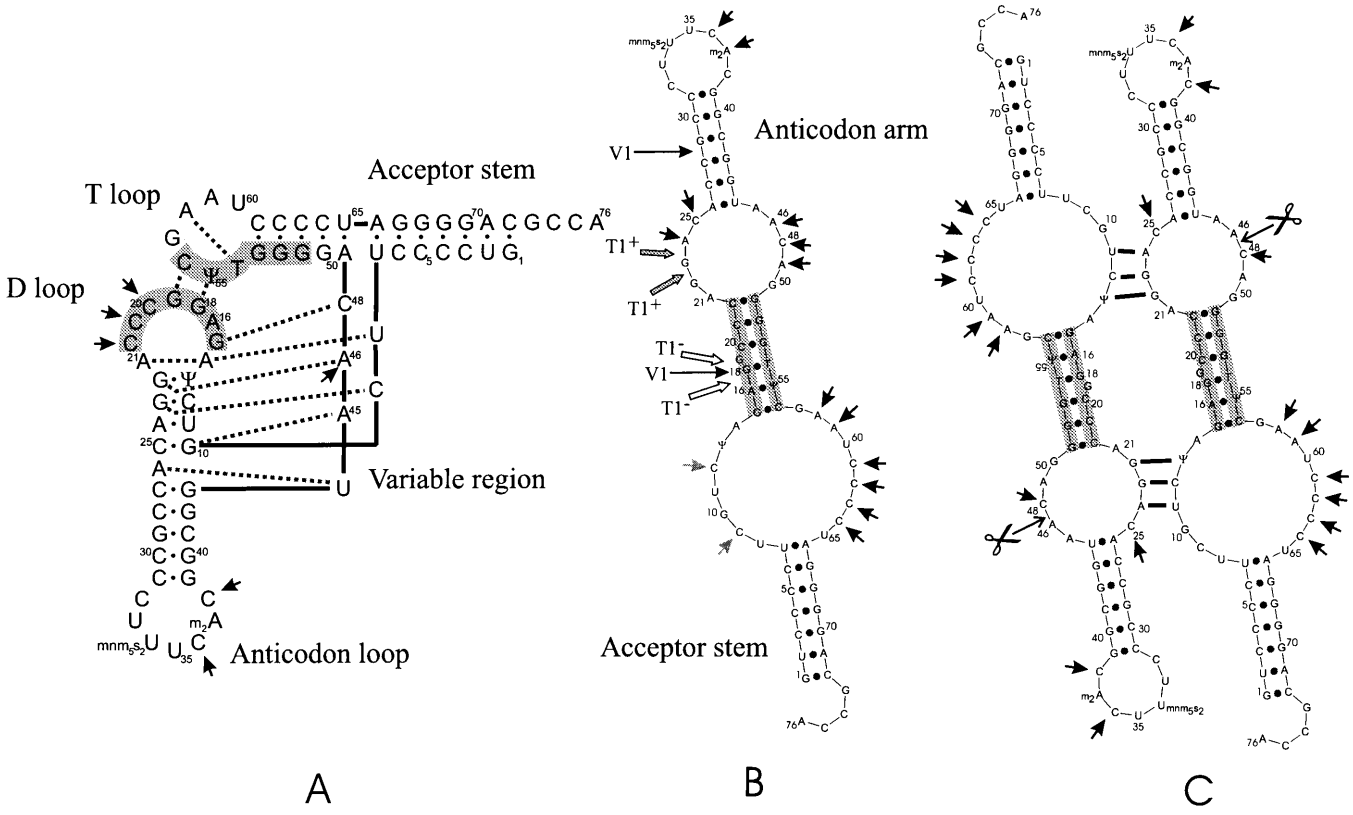

Figure 3. Proposed structures of the native, inactive and dimeric conformers of *E.coli* $tRNA^{Glu}$. Positions reactive to DEPC or DMS are highlighted by arrows. (**A**) Schematic L-shaped structure of the native *E.coli* $tRNA^{Glu}$ deduced from the crystallographic structures of yeast $tRNA^{Phe}$ and yeast $tRNA^{Asp}$ (24); (**B**) secondary structure model for the inactive conformer of $tRNA^{Glu}$, derived from the data obtained by DEPC, DMS, RNase V1 and RNase T1 (22) probing (Fig. 1); (**C**) probable structure of the dimer. Black arrows indicate accessible nucleotides at 25°C (or 4°C for the dimer) and gray arrows indicate additional accessible nucleotides at 50°C. Long black arrows with a V1 tag indicate major RNase V1 cuts. Large arrows with $T1^+$ or $T1^-$ tags indicate regions more or less susceptible to RNase T1 in the inactive form than in the native one. Scissors show C–A fragile bonds specific to the dimer. Gray shadows underline nucleotides from the native tRNA involved in alternative base pairings in the inactive foldings.

indicates that under these conditions the cloverleaf form must be far less stable than the hairpin. The A37 susceptibility in the absence of Mg^{2+} indicates that this ion plays a role in the correct folding of the anticodon loop; whatever this alteration is, it does not affect the formation of a complex with $tRNA^{Phe}$ via an anticodon–anticodon interaction (12).

The rigid elements present in this model of the secondary structure of the inactive conformer are three short helices (Fig. 3B). The fact that the electrophoretic mobility of the inactive conformer is 10% higher than that of the native conformer near 0°C (12) suggests that its tertiary structure is more compact than that of the active conformer. Moreover, the fact that the inactive conformer is eluted earlier than the native one from the positively charged and rigid resin RPC-5 (10) suggests that the former has shorter negatively charged rigid sections; this is analogous to the stronger binding of double-stranded than of single-stranded DNA to hydroxyapatite (23,24; for a review see 25). These two properties are consistent with our model where shorter rigid elements are present in the inactive conformer than in the native one, which contains two helices of 11 and 12 bp, respectively (Fig. 3A).

From their NMR study on the inactive conformer of *E.coli* $tRNA^{Glu}$, Bina-Stein *et al.* (13) concluded that the transition from the native to the inactive conformation can be interpreted as a change of tertiary structure (loss of tertiary interaction followed by the formation of new bonds) and probably loss of the D-stem. For the same transition, Eisinger and Gross (12) measured an activation energy of 64 kcal/M, which corresponds to loss of at least 20 stacked base pairs. In our model, based on the results of probing with DMS, DEPC and RNase V1 (Fig. 3), melting of the T- and D-stems would contribute about half of this energy barrier (10 bp) and the difference would come from the loss of tertiary structure, which in yeast $tRNA^{Phe}$ is mediated by about 10 stacking and pairing interactions. Therefore, this model accounts better for the measured native to inactive activation energy than would unfolding of only the D-stem and the tertiary structure. It also agrees with the relaxation kinetics data that were interpreted by a structure with three helical segments (13).

Eisinger and Gross (12) observed that the transition from the native to the inactive conformation causes 1–2% hyperchromicity. Knowing that the total unfolding of $tRNA^{Glu}$

causes 25% hyperchromicity (26), we estimate that the inactive form loses three to six stacking interactions. Taking into account that native $tRNA^{Glu}$ may contain about four bases that are not stacked (as in $tRNA^{Phe}$, excluding the CCA 3'-end), we should have a total of 7–10 unstacked bases in the inactive conformer. In our model, we identified six of them: A24, A46, A49, A58 and A59, which are accessible to DEPC, and the bulging G19, which must be excluded from the central helix.

Structure of the inactive $tRNA^{Glu}$ dimer

The inactive conformer of $tRNA^{Glu}$ forms a dimer in the presence of Mg^{2+} ions at low temperature (12). The only difference between the digestion patterns of this dimer and that of the monomeric denatured conformer is that A24 is protected in the former (Fig. 2). This protection may come from tertiary interactions present at 4°C but absent at 25°C or from interactions involved in dimer formation. An additional difference between the monomeric and dimeric forms of the inactive tRNA concerns the absence and presence, respectively, of a strong degradation site around nucleotide 46. As the energy barrier for formation of the dimer from the inactive conformer is only 14 kcal/M (12), it is likely that very few changes occurred in the secondary structure of the inactive conformer during its dimerization. Therefore, dimer formation probably occurs by pairing of bases located in the loops of the hairpin structure. One possibility which would account for the protection of A24 is an antiparallel alignment of two hairpins interacting by the following base pairs: G22–Ψ'13, G23–C'12 and A24–U'11 and, reciprocally, G'22–Ψ13, G'23–C12 and A'24–U11 (Fig. 3C). Dimerization of several tRNAs has been observed in the presence of their cognate codons (27); it was also observed in the absence of codons for several *in vitro* tRNA gene transcripts (28,29).

General discussion

The present investigation clearly shows a novel RNA fold for the inactive $tRNA^{Glu}$ from *E.coli* that differs markedly from the canonical cloverleaf. This study confirms and strengthens previous data suggesting that the inactive molecule has undergone dramatic changes rather than faint conformational changes within the cloverleaf. In the experimentally established fold, novel base pairings are formed between complementary sequences in the D-loop and nucleotides from the T-arm (Fig. 3, gray nucleotides). The two structural elements shared by the native and the inactive conformers are the acceptor stem and the anticodon arm; these are also the regions that contain most identity elements of tRNA for aminoacyl-tRNA synthetases (reviewed in 30,31). On the other hand, the two major identity elements of *E.coli* $tRNA^{Glu}$ (U11–A24 and Ψ13–G22–A46) are located in the extended D-arm (32). These interactions are totally disrupted in our model, which thus correlates with the lack of acceptor activity of this inactive conformer for glutamate.

In their groundbreaking report of the first known nucleotide sequence of a nucleic acid, Holley *et al*. (33) proposed three possible conformations for yeast $tRNA^{Ala}$; one of them is a hairpin with several internal loops and another is the clover leaf. The possibility of the hairpin model was soon eliminated by the analysis of X-ray scattering at small angles (34). No hairpin structures were proposed for tRNA before the observation by X-ray diffraction of the L-shaped 3-dimensional structure of yeast $tRNA^{Phe}$ (reviewed in 35).

Almost all the known inactive conformers of other tRNAs are obtained at low magnesium concentration. Using the secondary structure prediction program *mfold* (19), we observed that the calculated structures for those tRNAs have little or no resemblance to the canonical cloverleaf (results not shown), which in most cases is thermodynamically unfavorable (this program does not take into account tertiary interactions). Therefore, these tRNAs require a ligand (usually Mg^{2+}) to acquire a conformation that can be aminoacylated, as others require post-transcriptional modification to reach this active conformation (2). In conclusion, this work suggests that biologically active forms of macromolecules, here a tRNA, are not necessarily fully imprinted in the gene of this molecule, but require additional information, in the present case a certain magnesium ion concentration. Whether this potential of $tRNA^{Glu}$ to fold into alternative structures has biological significance remains to be investigated.

ACKNOWLEDGEMENTS

We thank Dr Paul F. Agris and Mr Daniel Dubois for stimulating discussions and Dr Michael Zuker for his help in using the *mfold* software. This work was supported in part by grant OGP0009597 from the Natural Sciences and Engineering Research Council of Canada (NSERC) and grant 97-ER-2481 from the Fonds pour la Formation de Chercheurs et l'Aide à la Recherche du Québec (FCAR) to J.L. and in part by grants from the Centre National de la Recherche Scientifique (CNRS), the Ministère de l'Enseignement Supérieur et de la Recherche (MESR) and Université Louis Pasteur (Strasbourg). E.M. was a postgraduate fellow of NSERC and FCAR.

REFERENCES

1. Ellis,R.J. (ed.) (1996) *The Chaperonins*, Cell Biology A Series of Monographs. Academic Press, San Diego, CA.
2. Helm,M., Brule,H., Degoul,F., Cepanec,C., Leroux,J.P., Giegé,R. and Florentz,C. (1998) *Nucleic Acids Res.*, **26**, 1636–1643.
3. Lindahl,T., Adams,A. and Fresco,J.R. (1966) *Proc. Natl Acad. Sci. USA*, **55**, 941–948.
4. Adams,A., Lindahl,T. and Fresco,J.R. (1967) *Proc. Natl Acad. Sci. USA*, **57**, 1684–1691.
5. Fresco,J.R., Adams,A., Ascione,R., Henley,D. and Lindahl,T. (1966) *Cold Spring Harbor Symp. Quant. Biol*., **31**, 527–537.
6. Ishida,T. and Sueoka,N. (1967) *Proc. Natl Acad. Sci. USA*, **58**, 1081–1087.
7. Lindahl,T., Adams,A. and Fresco,J.R. (1967) *J. Biol. Chem.*, **242**, 3129–3134.
8. Ishida,T., Snyder,D. and Sueoka,N. (1971) *J. Biol. Chem.*, **246**, 5965–5969.
9. Nishimura,S. (1971) In Cantoni,G.L. and Davies,D.R. (eds), *Procedures in Nucleic Acid Research*. Harper and Row, New York, NY, Vol. 2, pp. 542–564.
10. Tremblay,T.-L. and Lapointe,J. (1986) *Biochem. Cell Biol*., **64**, 315–321.
11. Blattner,F.R. *et al*. (1997) *Science*, **277**, 1453–1474.
12. Eisinger,J. and Gross,N. (1975) *Biochemistry*, **14**, 4031–4041.
13. Bina-Stein,M., Crothers,D.M., Hilbers,C.W. and Shulman,R.G. (1976) *Proc. Natl Acad. Sci. USA*, **73**, 2216–2220.
14. Bischoff,R. and McLaughlin,L.W. (1985) *Anal. Biochem.*, **151**, 526–533.
15. Silberklang,M., Gillum,A.M. and RajBhandary,U.L. (1979) *Methods Enzymol*., **59**, 58–109.
16. Keith,G. (1995) *Biochimie*, **77**, 142–144.
17. Romby,P., Moras,D., Dumas,P., Ebel,J.P. and Giegé,R. (1987) *J. Mol. Biol.*, **195**, 193–204.
18. Lowman,H.B. and Draper,D.E. (1986) *J. Biol. Chem.*, **261**, 5396–5403.
19. Walter,A.E., Turner,D.H., Kim,J., Lyttle,M.H., Muller,P., Mathews,D.H. and Zuker,M. (1994) *Proc. Natl Acad. Sci. USA*, **91**, 9218–9222.
20. Peattie,D.A. and Gilbert,W. (1980) *Proc. Natl Acad. Sci. USA*, **77**, 4079–4082.

21. Hosaka,H., Ogawa,T., Sakamoto,K., Yokoyama,S. and Takaku,H. (1991) *FEBS Lett.*, **293**, 204–206.
22. Wrede,P., Wurst,R., Vournakis,J and Rich,A. (1979) *J. Biol. Chem.* **254**, 9608–9616.
23. Martinson,H.G. (1973) *Biochemistry*, **12**, 2731–2736.
24. Kawasaki,T., Ikeda,K., Takahashi,S. and Kuboki,Y. (1986) *Eur. J. Biochem.*, **155**, 249–257.
25. Broadhurst,A.V. (1997) In *Current Protocols in Protein Science*. John Wiley & Sons, New York, NY, Vol. 1, unit 8.6.
26. Lapointe,J. and Söll,D. (1972) *J. Biol. Chem.*, **247**, 4975–4981.
27. Labuda,D. and Porschke,D. (1983) *J. Mol. Biol.*, **167**, 205–209.
28. Kholod,N., Pan'kova,N., Ksenzenko,V. and Kisselev,L. (1998) *FEBS Lett.*, **426**, 135–139.
29. Kholod,N., Vassilenko,K., Shlyapnikov,M., Ksenzenko,V. and Kisselev,L. (1998) *Nucleic Acids Res.*, **16**, 2500–2501.
30. McClain,W.H. (1995) In Söll,D. and RajBhandary,U.L. (eds), *tRNA Structure, Biosynthesis and Function*. ASM Press, Washington, DC, pp. 335–347.
31. Giegé,R., Sissler,M. and Florentz,C. (1998) *Nucleic Acids Res.*, **26**, 5017–5035.
32. Sekine,S., Nureki,O., Sakamoto,K., Niimi,T., Tateno,M., Go,M., Kohno,T., Brisson,A., Lapointe,J. and Yokoyama,S. (1996) *J. Mol. Biol.*, **256**, 685–700.
33. Holley,R.W., Apgar,J., Everett,G.A., Madison,J.T., Marquise,M., Merril,S.H., Penswick,J.R. and Zamir,R. (1965) *Science*, **147**, 1462–1465.
34. Lake,J.A. and Beeman,W.W. (1968) *J. Mol. Biol.*, **31**, 115–125.
35. Ebel,J.P. (1973) In Sadron,C. (ed.), *Dynamic Aspects of Conformational Changes in Biological Macromolecules*. D. Reidel Publishing Co., Dordrecht, Holland, pp. 301–326.